applied sciences

MDPI

Article

Molecular Insights into the Interactions Between Human Serum Albumin and Phospholipid Membranes

Maciej Przybyłek [1,*], Piotr Bełdowski [2], Damian Ledziński [3], Zbigniew Lutowski [3], Adam Mazurkiewicz [4], Przemysław Raczyński [5], Andra Dedinaite [6] and Per M. Claesson [7]

1 Department of Physical Chemistry, Pharmacy Faculty, Collegium Medicum of Bydgoszcz, Nicolaus Copernicus University in Toruń, Kurpińskiego 5 Street, PL-85096 Bydgoszcz, Poland
2 Institute of Computer Science, Kazimierz Wielki University in Bydgoszcz, Kopernika 1, PL-85074 Bydgoszcz, Poland; piotr.beldowski.pb@gmail.com
3 Faculty of Telecommunications, Computer Science and Electrical Engineering, Bydgoszcz University of Science and Technology, Kaliskiego 7 Street, PL-85796 Bydgoszcz, Poland; damian.ledzinski@pbs.edu.pl (D.L.); zbigniew.lutowski@pbs.edu.pl (Z.L.)
4 Faculty of Mechanical Engineering, Bydgoszcz University of Science and Technology, Kaliskiego 7 Street, PL-85796 Bydgoszcz, Poland; adam.mazurkiewicz@pbs.edu.pl
5 Faculty of Science and Technology, University of Silesia in Katowice, 75 Pułku Piechoty 1A, PL-41500 Chorzów, Poland; przemyslaw.raczynski@us.edu.pl
6 School of Engineering Sciences in Chemistry, Biotechnology and Health, Engineering Pedagogics, KTH Royal Institute of Technology, SE-10044 Stockholm, Sweden; andra@kth.se
7 Division of Surface and Corrosion Science, Department of Chemistry, KTH Royal Institute of Technology, SE-10044 Stockholm, Sweden; percl@kth.se
* Correspondence: m.przybylek@cm.umk.pl

Abstract: In this study, molecular dynamics simulations were employed to analyze interactions between phospholipid membranes and human serum albumin (HSA) in the presence of mono- and divalent cations. Two types of membranes, composed of dipalmitoyl phosphatidylcholine (DPPC) and dipalmitoyl phosphatidylethanolamine (DPPE), were utilized. The results revealed that both systems exhibited high stability. The DPPE complexes displayed a greater affinity for albumin compared to DPPC. The high stability of the complexes was attributed to a high number of ionic contacts and hydrogen bonds. The presence of mono- and divalent metal cations significantly influenced the membrane's capacity to bind proteins. However, these effects varied depending on the phospholipid composition of the bilayer. The studies confirmed the relatively low ability of DPPC to bind potassium ions, as previously observed by others. Consequently, the DPPC/HSA/K^+ complex was found to be the least stable among the systems studied. While DPPC interactions were limited to HSA domains I and II, DPPE was able to interact with all domains of the protein. Both lipid bilayers exhibited substantial structural changes and characteristic curvature induced by interactions with HSA, which confirms the formation of relatively strong interactions capable of influencing the arrangement of the phospholipids.

Keywords: phospholipid membranes; DPPC; DPPE; human serum albumin; intermolecular interactions; hydrogen bonds; ionic interactions; mono- and divalent cations; molecular dynamics

Citation: Przybyłek, M.; Bełdowski, P.; Ledziński, D.; Lutowski, Z.; Mazurkiewicz, A.; Raczyński, P.; Dedinaite, A.; Claesson, P.M. Molecular Insights into the Interactions Between Human Serum Albumin and Phospholipid Membranes. *Appl. Sci.* **2024**, *14*, 11753. https://doi.org/10.3390/app142411753

Academic Editor: Gang Wei

Received: 29 October 2024
Revised: 13 December 2024
Accepted: 13 December 2024
Published: 17 December 2024

1. Introduction

Phospholipid bilayers play a crucial role in organisms by constituting the basic structure of cell membranes, providing a barrier against environmental factors, and facilitating various cellular processes [1–3]. Despite their well-known biological role and relatively simple structure, phospholipids remain a subject of scientific interest for their emerging applications and features, such as learning and memory capabilities [3]. Notably, reconstituted proteoliposomes also merit special consideration for their ability to replicate natural biological systems, particularly in bioenergy applications [4] and artificial cell models [5].

Two classes of phospholipids with significant biological relevance are phosphatidylcholine (PC) and phosphatidylethanolamine (PE), with representative examples being 1,2-dipalmitoyl-sn-glycero-3-phosphatidylcholine (DPPC) and 1,2-dipalmitoyl-sn-glycero-3-phosphorylethanolamine (DPPE). Membranes and liposomes composed of DPPC and DPPE are widely utilized in pharmaceutical and biomedical applications [3,6–12]. DPPE membranes exhibit denser packing compared to those formed from DPPC, influencing their interactions with other molecules [13,14].

A far more complex biomolecule than DPPE and DPPC, which also holds significant biological and biomedical importance, is human serum albumin (HSA). Similar to phospholipids, HSA has the ability to bind with a wide range of both polar and non-polar substances, highlighting its versatile functional properties [15,16]. Moreover, it plays crucial biological roles, serving as a carrier for various bioactive molecules, maintaining osmotic pressure, pH of blood, and electrolyte homeostasis [17–21]. The interactions between HSA and phospholipid layers significantly affect molecular transport, as demonstrated in both in vitro and in vivo studies [22]. It is worth mentioning that albumins are known to possess multiple binding sites when interacting with phospholipid liposomes [23]. Notably, even a low concentration of bovine serum albumin can modulate the structural arrangement of phospholipids [24].

Lipid–protein systems have a wide range of applications in various fields, such as encapsulation [25], food packaging, and coatings [26–28]. The distinctive properties of phospholipid- and albumin-based systems have made them valuable in drug delivery. This has been particularly evident in the development of nanocomplexes and nanoparticles, which enable the controlled and sustained release of active substances [29,30]. In addition to the well-established biological and pharmaceutical significance of HSA-membrane interactions, their biomechanical implications also warrant attention. Phospholipids, along with HSA, γ-globulin, collagen, lubricin, and hyaluronan, are components of articular cartilage and synovial fluid, contributing significantly to joint lubrication and health [31].

In previous works [32–37], the interactions between phospholipid assemblies and various natural and synthetic macromolecules were examined using molecular dynamics methods. Particularly interesting for understanding the mechanism of binding biologically active compounds to biopolymers and membranes is the role of physiologically occurring ions such as Na^+, K^+, Mg^{2+}, and Ca^{2+}. It is well-known that they can significantly influence the structural organization and energetic stability of various biomolecular systems [36,38–41]. The next phase of the project involves exploring the interactions of HSA with DPPC and DPPE phospholipid bilayers, which contain choline and ethanolamine groups, respectively. Although the ability of albumin and other serum proteins to bind to lipid bilayers has been investigated [42], to the best of our knowledge, there are no available studies on the impact of changes in the phospholipid headgroup structure on albumin affinity to the membrane. The influence of metal ions on phospholipid stability has been investigated extensively [43–47]. However, a comprehensive analysis of their effects on DPPC and DPPE bilayers, particularly in the context of interactions with HSA, remains lacking. This molecular dynamics simulation study aims to fill the mentioned gaps by analyzing the affinity of HSA for phospholipid bilayers of DPPC and DPPE and the influence of Na^+, K^+, Mg^{2+}, and Ca^{2+} cations.

2. Methods

In this study, all-atom molecular dynamics (MD) simulations employing the NPT ensemble were conducted utilizing the AMBER14 force field [48] to investigate the intermolecular interactions between human serum albumin (HSA) and bilayers composed of either 1,2-dipalmitoyl-sn-glycero-3-phosphorylcholine (DPPC) or 1,2-dipalmitoyl-sn-glycero-3-phosphorylethanolamine (DPPE). The HSA structure (PDB code: 1e78) was obtained from the Protein Data Bank [49] and subjected to structural refinement procedures. Specifically, missing hydrogen atoms were added using the YASARA software (2021) [50], followed by homology modeling to incorporate absent amino acids based on the PDB struc-

ture and secondary structure prediction protocols. The resulting HSA model considered for analysis exhibited a molecular mass of 66.5 kDa.

The DPPC and DPPE bilayers, each comprising 700 lipids, were constructed and initially equilibrated utilizing the CHARMM-GUI software platform (http://www.charmm-gui.org, accessed on 1 March 2023) [51–53]. Subsequently, a 10-nanosecond (ns) equilibration period was employed to mitigate potential atomic clashes within the membrane. Following equilibration, the HSA molecule was introduced adjacent to the bilayer surface without perturbing its structural integrity. Ten unique orientations of HSA were randomly positioned approximately 0.5 nm from the bilayer surface to explore potential binding sites.

Initial MD simulations spanning 100 ns have been performed to select the most stable binding sites. DPPC showed more specific HSA domain binding affinity, resulting in protein desorption from the surface (except for those orientations involving mostly domain II). DPPE membrane formed stable complexes with HSA regardless of the orientation. After this initial period, binding was retained in only five DPPC systems. Therefore, further analyses and computations included only the five most stable structures for both DPPE/HSA and DPPC/HSA systems. For this reason, the simulations for selected structures were repeated and extended to 200 ns. Periodic boundary conditions were enforced to simulate an "infinite" bilayer, and the TIP3P water model [54,55] was employed.

All simulations were conducted under physiological conditions (temperature: 310 K, pH: 7.0, P = 1 Atm, NPT procedure [50,56]) employing a 2 fs time step. Two scenarios were investigated: (i) HSA at the bilayer interfaced with an aqueous solution of NaCl and (ii) HSA at the bilayer interfaced with a $CaCl_2$ aqueous solution. Additionally, simulations with KCl and $MgCl_2$ solutions were also performed. Each simulation box encompassed water, a single HSA molecule, a DPPC/PE bilayer, 240 cations for bivalent ions, and around 480 cations for monovalent ions, along with an appropriate number of anions to maintain electroneutrality. The default ion parameterization in YASARA was applied throughout the study.

The equilibrium state of the system was achieved after approximately 40 ns, following which simulations were continued for an additional 200 ns to gather data. To maintain constant pressure and temperature throughout the simulations, we utilized a modified Berendsen barostat and thermostat [57], each with a relaxation time of 1 fs.

Analysis of the MD simulations involved the evaluation of binding free energies, the formation of hydrogen bonds, and ionic interactions. These interactions were elucidated through contact maps illustrating the frequency of specific molecular pairings. Furthermore, the distribution of water molecules surrounding the HSA–bilayer complexes, as well as the distribution of calcium and sodium ions, were analyzed to provide insights into the solvation environment and potential ion-mediated interactions.

2.1. Free Energy of Binding

The binding free energy was determined by applying the single trajectory method, employing Molecular Mechanics/Poisson–Boltzmann Surface Area (MM/PBSA) [58] and YASARA Structure. The solvation energy and electrostatic interactions were analyzed using the AMBER14 force field combined with the Adaptive Poisson–Boltzmann Solver (APBS) [59]. The electrostatic surface potential map was generated through this approach. Utilizing the optimized structures, the binding free energy, ΔG_b, was computed using the following equation:

$$\Delta G_b = \Delta G_c - (\Delta G_m + \Delta G_{HSA}) \quad (1)$$

where ΔG_c, ΔG_m, and ΔG_{HSA} represent the minimized free energies of the HSA-membrane complex, membrane, and HSA, respectively. The total ΔG_b has multiple contributions, which under isothermal conditions can be represented by Equation (2):

$$\Delta G_b = \Delta H_{HSA-membrane} + \Delta H_{PS} + \Delta H_{NS} - T\Delta S \quad (2)$$

where $T\Delta S$ represents the conformational entropy contribution and $\Delta H_{HSA\text{-}membrane}$ denotes the interaction enthalpy between the HSA and the phospholipid bilayer. This component encompasses both electrostatic and van der Waals interactions. The terms ΔH_{PS} and ΔH_{NS} denote the polar and non-polar solvation enthalpies, respectively.

2.2. Intermolecular Contacts Identification

In this study, the default YASARA settings for crucial intermolecular contact identification were utilized.

As is well known, one of the most important interactions stabilizing biological systems is hydrogen bonding. According to the applied definition, they are strong interactions considered to be formed when the contact energy exceeds 6.25 kJ/mol, representing 25% of the optimal value of 25 kJ/mol [60]. The bond energy in kJ/mol is calculated as a function of the hydrogen acceptor distance and two scaling factors using the following formula [61]:

$$E_{HB} = 25 \cdot \frac{2.6 - \max(Dis_{H-A}, 2.1)}{0.5} \cdot Scale_{D-A-H} \cdot Scale_{H-A-X} \quad (3)$$

The first scaling factor ($Scale_{D-A-H}$) depends on the angle formed by the donor-hydrogen-acceptor. The second scaling factor ($Scale_{D-A-H}$) is derived from the angle formed by the hydrogen-acceptor-X, where X represents the atom covalently bound to the acceptor.

The other important intermolecular forces, namely ionic interactions, occur when oppositely charged ions localized on specific atoms are close in space. These interactions, along with hydrogen bonds, constitute the primary contribution to stabilizing the systems in question. The definition of ionic interactions involves a two-atom contact determined by the distance between formal centers of integer charges.

It is worth mentioning that using the default YASARA settings, an attempt was made to characterize the hydrophobic interactions. These weak molecular forces are defined as the contacts between specific groups recognized as hydrophobic, such as $–CH_3$ or $–CH_2–$. However, their contribution to complexation at the key sites between the polar phospholipid heads and the residues in HSA was found to be negligibly small (<1%).

3. Results and Discussion

This research investigates the energetic and structural consequences of complex formation between HSA and phospholipid membranes (DPPC and DPPE). It details the changes in phospholipid layers resulting from interactions with HSA, examining the protein's affinity for the studied membranes, the geometric and energetic parameters of molecular contacts, and their distribution in the presence of Na^+, K^+, Mg^{2+}, and Ca^{2+} ions.

3.1. The Effect of HSA Binding on Bilayer Shape and Density

An important feature of phospholipids from a biological perspective is their ability to self-organize, which can, of course, be influenced by the presence of other compounds. The optimized structures of three examples of molecular assemblies containing albumin and considered phospholipid membranes are presented in Figure 1. Additionally, snapshots of the simulation boxes at the conclusion of the simulation are provided in the Supplementary Materials (Figure S1).

It is worth noting that at 310 K, a temperature close to physiological conditions, fully hydrated bilayers composed of DPPC and DPPE are in the gel phase [62]. As clearly illustrated in the snapshots, although the obtained membranes maintain a well-ordered structure, as seen in the images, the membrane undergoes a shape change to accommodate HSA. The interaction between phospholipid bilayers and proteins, including albumin, has been extensively studied and is well documented both experimentally and theoretically [63–68]. These interactions often result in notable surface deformations of the bilayers, driven by the minimization of the overall free energy of the system. This process leads to significant alterations in the curvature and structural integrity of the lipid bilayer at the site of contact with the protein. Albumins,

owing to their unique structural properties and affinity for phospholipid liposomes [23], can induce complex changes within the bilayer. It is worth mentioning that experimental research on the systems composed of phosphatidylcholine (PC) and sodium cholate has revealed that the concentration of albumin can significantly affect the size of micelles [69]. Furthermore, Al-Ayed [70] has demonstrated the critical role of bovine albumin in the solubilization and phase transitions of systems composed of dipalmitoylphosphatidylcholine (DPPC). These studies suggest the presence of strong, specific interactions between albumin and the membrane surface, which can lead to considerable changes in the physical properties of the membrane. Such findings contribute to a deeper understanding of the dynamic nature of membrane-protein interactions and their implications for cellular processes and membrane functionality. It is suggested that the ability of the cell membrane to transport essential cellular components may be influenced by its strong interaction with albumin [22].

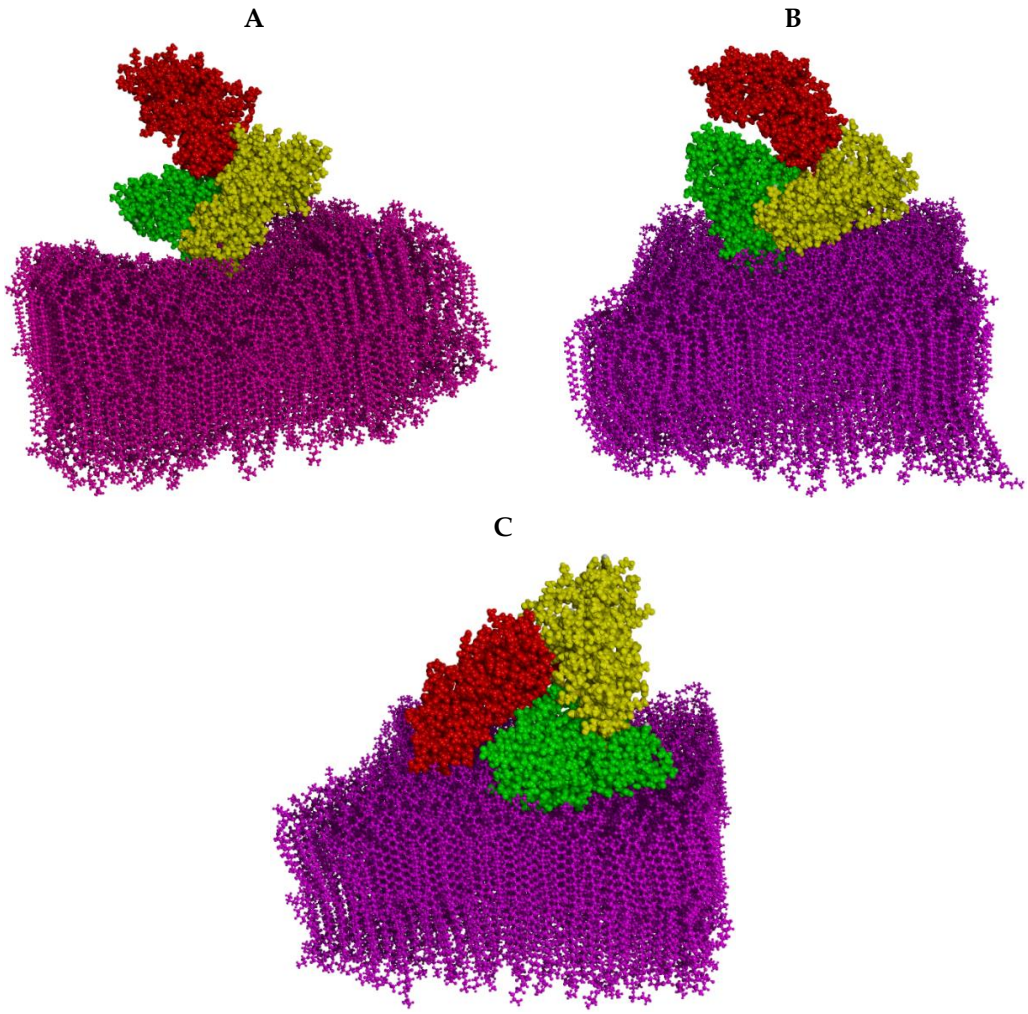

Figure 1. Preferred orientations of HSA concerning the phospholipid bilayer, illustrated by selected snapshots of complexes in the presence of Ca^{2+} cations. The membrane is colored pink, HSA domains: I—green, II—yellow, III—red. Panel (**A**) shows the preferred arrangement of HSA on the DPPC membrane. Panels (**B**) and (**C**) present the two possible orientations of HSA with respect to the DPPE membrane.

The permeability of membranes can be significantly influenced by the deposition density of phospholipids [71,72]. It is noteworthy that the effect of reduced liposome packing due to interactions with serum proteins has been described using experimental tools by Bonté and Juliano [42]. Additionally, research by Melcrová et al. [72] demonstrated that the presence of calcium salts can affect the packing of phospholipids in the membrane.

To characterize the impact of complex formation on structural changes in the phospholipid bilayer, the changes in phospholipid density resulting from the adsorption of HSA on its surface were analyzed. Figure 2 presents selected phospholipid mass profiles as a function of cross-section for selected systems. The plots represent average density values across the entire bilayer. Additionally, the density profiles for the nitrogen atoms in the phospholipid head groups are also depicted. As clearly seen, the formation of a complex with HSA affects the distances between phospholipid molecules in the considered membranes. Interestingly, when focusing on the nitrogen atoms in the phospholipid head groups, only minor variations in density are observed. For example, the difference between the maximum and minimum mass density values for DPPE phospholipid head group nitrogens is approximately 400 (Figure 2B), whereas the difference for the average mass density across all atoms in the membrane exceeds 10,000. Despite these small variations in mass density, the shape of the profiles for nitrogen atoms differs significantly between membranes composed of DPPC and DPPE.

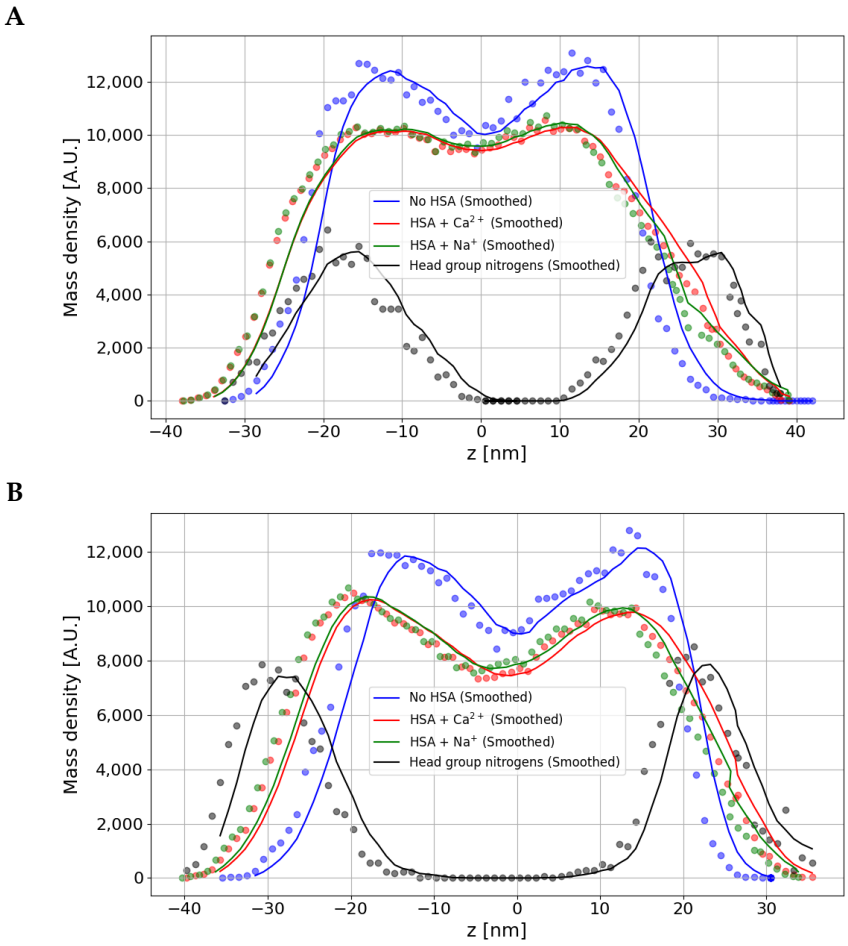

Figure 2. The effect of HSA adsorption on mass profiles of DPPC (**A**) and DPPE (**B**) phospholipid bilayers. The z-parameter denotes the distance from the membrane center. Smoothed plots were obtained using a moving average. The mass density values of head group nitrogens were scaled by a factor of 20 due to their low magnitude.

3.2. The Affinity of HSA for DPPC and DPPE in the Presence of Mono- and Divalent Cations

The types of molecular contacts discussed in this study are presented in Figure 3. As shown, the examined systems are primarily stabilized by hydrogen bonds and ionic interactions formed by the hydrophilic heads of phospholipids and specific residues in HSA.

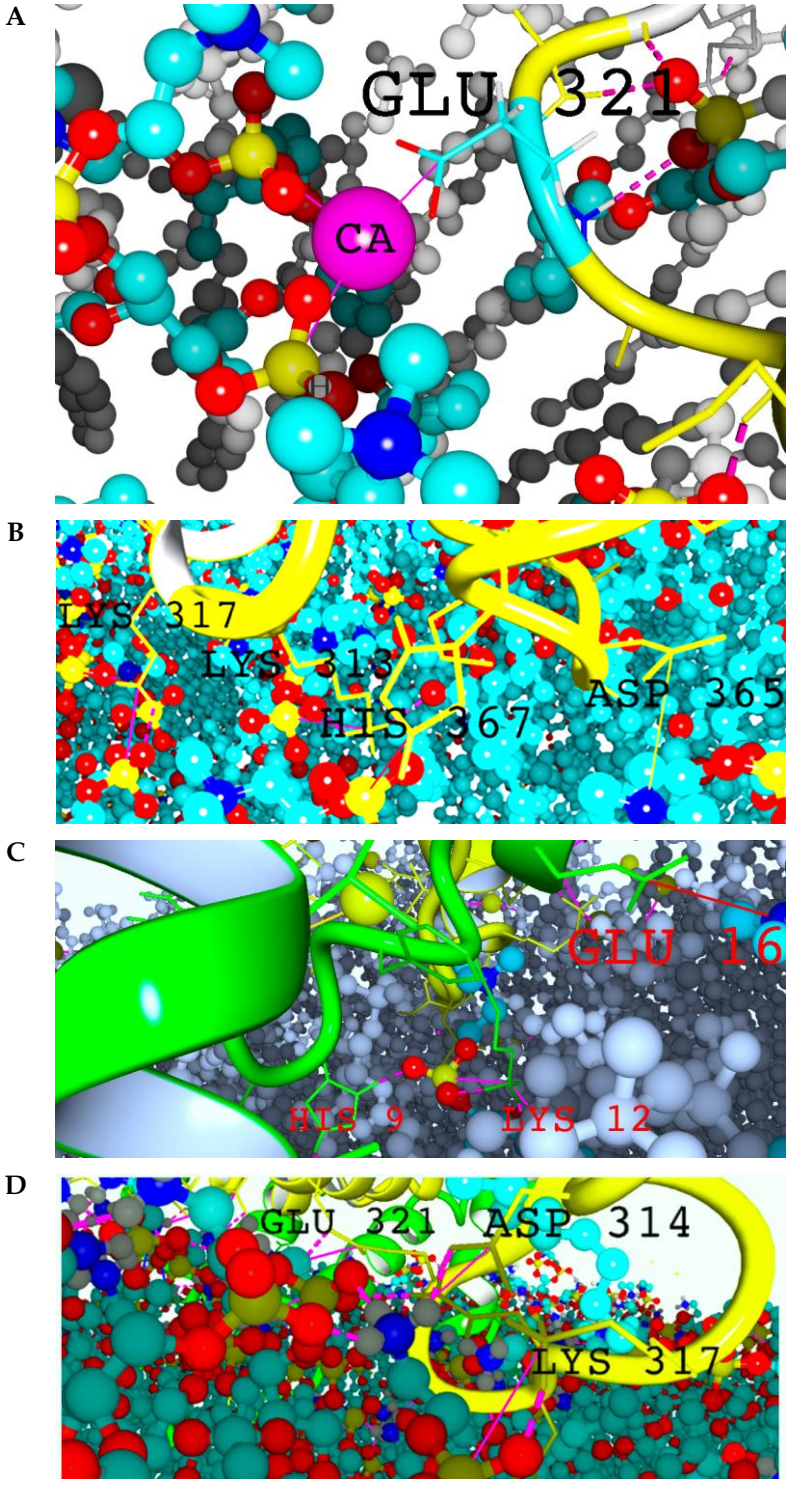

Figure 3. Examples of key membrane–HSA interactions are DPPC/HSA (**A**,**B**) and DPPE/HSA (**C**,**D**). Pink solid lines indicate ionic interactions. Dotted pink—H-bonds. Atoms of lipids are presented in ball-like models and colored in the following fashion: turquoise—carbon, red—oxygen, blue—nitrogen, and yellow—phosphorus. The calcium cation is represented by a pink ball. Large yellow balls indicate magnesium ions. Solid lines with additional side groups in a stick-like model represent the HSA molecule. Its color corresponds to the domains depicted in Figure 1. The panels highlight interactions with specific residues in HSA: Panel A: GLU 321; Panel B: LYS 317, LYS 313, HIS 367, and ASP 365; Panel C: HIS 9, LYS 12, and GLU 16; Panel D: GLU 321, ASP 314, and LYS 317.

Given the polyelectrolytic nature of proteins, the distribution of electrostatic charge within the molecule, dictated by pH, determines the type and number of intermolecular interactions they form. It is well known that albumin, which is characterized by an isoelectric point of c.a. 5, is negatively charged under physiological pH conditions (pH ≈ 7) [73,74]. As expected, the hydrophilic head groups of the phospholipid membranes interact with albumin through the ionic interactions formed by positively charged ammonium groups and negatively charged GLU and ASP residues (Figure 3). The other important interactions are hydrogen bonds formed by HIS and LYS residues, with the phosphate group playing the accepting role.

It is of significant importance to examine the energetic aspects, which reveal substantial differences in the mutual affinity of membranes and HSA. In Figure 4, the distribution of binding energy values determined for the complexes in the presence of Na^+, K^+, Ca^{2+}, and Mg^{2+} cations is presented. The confirmation that stable optimal structures were obtained is provided by the plot of root mean square deviation (RMSD) versus time (Figure 5). Additional trajectories are presented in Figures S2–S5 (Supplementary Materials). The trajectory analysis is useful for determining the equilibrium state, as indicated by a plateau. The attainment of a stable conformation is clearly observed both for the entire structure, as evidenced by considering the binding energy as a function of time (Supplementary Figure S1), and for individual binding sites (Supplementary Figure S2). In the latter case, however, broader thermal fluctuations and generally lower binding energy values are observed for DPPC compared to DPPE. For structures that have reached equilibrium, the binding energy values further suggest a higher affinity of HSA for the membrane composed of DPPE (Figure 4). The average binding energy values for DPPC in complexes containing Na^+, K^+, Ca^{2+}, and Mg^{2+} are 700, 600, 1300, and 1100 kJ/mol, while for DPPE, these values are 1800, 1400, 1800, and 1200 kJ/mol, respectively. Apart from energetic characteristics, changes in structural parameters during MD simulations serve as an indicator of system stability, as demonstrated in previous studies on protein-phospholipid bilayer interactions [75–78]. Minor variations in structural parameters suggest the formation of stable and energetically favorable interactions. As illustrated in Figure 5, the RMSD values of DPPC complexes with HSA are lower than those observed for DPPE complexes. It is noteworthy that, in simulations of DPPC/HSA in the presence of K^+ ions, two structures failed to reach equilibrium, resulting in complex dissociation. The destabilizing influence of K^+ is clearly reflected in the RMSD vs. time profile (Figure 5).

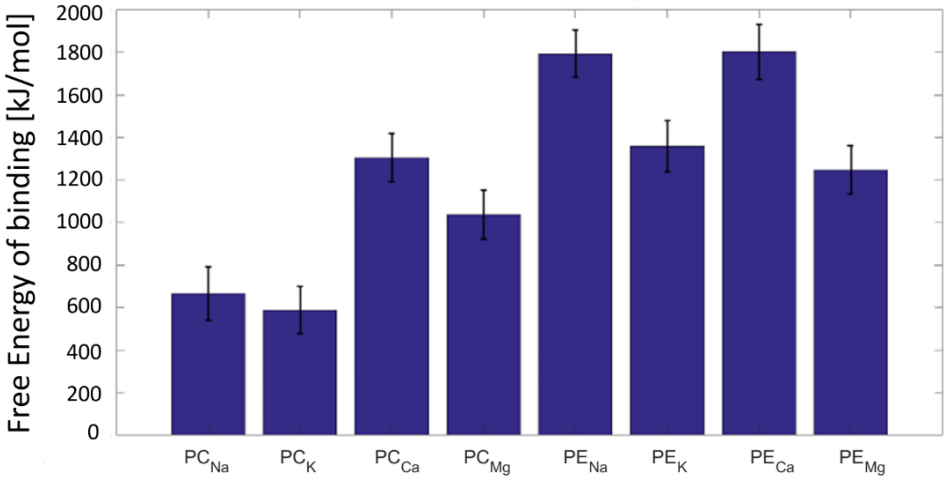

Figure 4. Bar plot showing the average free binding energy of HSA to the bilayer and its standard deviation for all cases studied. The symbols PC and PE represent the phospholipid membranes formed by DPPC and DPPE, respectively.

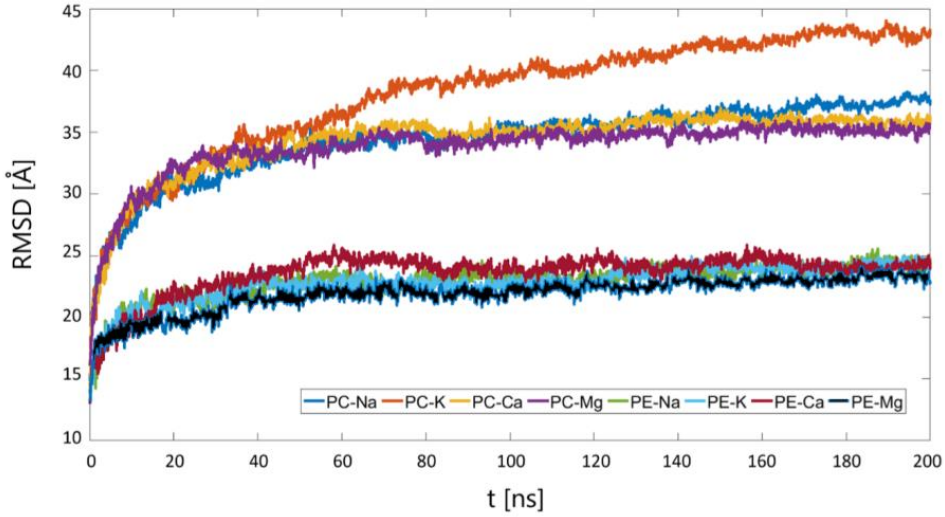

Figure 5. Root mean square deviation (RMSD) between the Cartesian atom coordinates in the two selections of HSA evolution in time. PC and PE symbols denote the phospholipid membranes formed by DPPC and DPPE, respectively.

As previous studies have shown [38], Na^+, Mg^{2+}, and Ca^{2+} impact the stability of complexes involving HSA. Notably, Ca^{2+} ions were found to be responsible for linking various peptides with phospholipid bilayers [79–81]. In contrast, Na^+ and K^+ ions are known to interact only slightly with albumin compared to Ca^{2+} and Mg^{2+} [82,83].

The binding of cations to phospholipids increases the positive charge of the bilayer, thereby promoting interactions with negatively charged albumin. Considering the atomic radius and ionic charge, the hydration ability of the studied ions increases as follows: $K^+ < Na^+ < Ca^{2+} < Mg^{2+}$, which aligns with experimental observations [84]. Ion hydration appears to be a competing effect against binding with phospholipids. On the other hand, the binding of ions of high positive charge (Mg^{2+}, Ca^{2+}) to the membrane is expected to promote stronger interactions with the negatively charged protein. However, as shown in Figure 4, this expectation is not met in the case of DPPE, as the presence of Mg^{2+} ions results in the weakest binding of HSA by the phospholipid bilayer. In the case of DPPC, an advantage of divalent ions in stabilizing the complex over monovalent ions can be observed, as the highest affinity for HSA was found in systems containing Ca^{2+} and Mg^{2+} ions. Notably, experimental data on the interactions of soybean lecithin with albumin support this observation [46]. PC phospholipids, including DPPC, are the main components of lecithins, contributing to their functional properties [85]. These phospholipids have been found to form efficient interactions with albumin [46,86,87]. The results of infrared spectroscopic measurements conducted by Tantipolphan et al. [46] have demonstrated that bovine serum albumin binds more effectively to hydrogenated soybean lecithin films in the presence of $CaCl_2$ compared to NaCl. On the other hand, the distributions of E_{bind} in the case of DPPE complexes containing Na^+ and Ca^{2+} cations are very similar. Further, both cations increase the stability of the complex when compared to K^+ and Mg^{2+}, respectively. For DPPC, complexes containing the K^+ ion exhibit the lowest stability. As previously mentioned, we have observed that two of these complexes disintegrate during the simulation period. Indeed, both experimental and theoretical studies conducted by other researchers [43–45,47] suggest a low affinity of K^+ for DPPC compared to other monovalent and divalent metal cations.

The stability of HSA-phospholipid complexes in the presence of mono- and divalent cations is primarily driven by ionic contacts between the phospholipid membrane and HSA, along with hydrogen bonds. However, the influence of ions on HSA affinity for the membrane appears to be more indirect than direct. It might seem that the differences in complex stability arise from the binding of components via ions. Nevertheless, ionic

bridges with Na^+, K^+, Mg^{2+}, and Ca^{2+} represent a negligible part of the interactions (<1%) compared to other types of molecular contacts, including direct ionic interactions between the phospholipid layer and the protein. In the DPPC/HSA system, ionic bridges are formed only between the phosphate group and the carboxyl group in GLU in the presence of Ca^{2+} ions, with an average distance between the atoms and the ion of 3.19 ± 0.14 Å. In the DPPE/HSA system, ionic bridges are formed by both GLU and ASP, characterized by distances of 3.33 ± 0.35 Å for GLU and 3.41 ± 0.25 Å for ASP.

The higher binding energy of HSA to the DPPE membrane, compared to DPPC, demonstrates greater mutual affinity of the components. This is attributed to structural differences in the phospholipid headgroup. As can be inferred from Figure 6, DPPE forms more direct ionic contacts (about 4–5 times) with HSA compared to DPPC. This is due to the difference in headgroup size and, consequently, the difference in positive charge density on groups capable of forming such contacts with HSA (-$N(Me)_3$ for DPPC and -NH_3 for DPPE) [88,89]. Additionally, the steric hindrances caused by the methyl groups in -$N(Me)_3$ may also play a role in influencing the stability of HSA associates formed by these lipids. Considering the effect of mono- and divalent cations on the individual complexes, significant differences are observed, regardless of whether DPPC or DPPE membranes are considered. The percentages of ionic interactions formed by particular residues and HSA domains are presented in Table S1 (Supplementary Materials). The highest percentage of ionic interactions in the case of DPPC (approximately half of all ionic interactions in the complex) is formed by LYS (48%, 45%, 47%, and 52% for the complexes with Ca^{2+}, Mg^{2+}, K^+, and Na^+, respectively). About 20% of the ionic interactions are formed by ASP or GLU. The contributions of ASP contacts are 20% (Ca^{2+}), 21% (Mg^{2+}), 20% (K^+), and 16% (Na^+), while for GLU contacts they are 25% (Ca^{2+}), 24% (Mg^{2+}), 24% (K^+), and 26% (Na^+). Noteworthy, a low number of ionic interactions (2–6%) was observed in the case of ARG and HIS. In the case of DPPE complexes with HSA, GLU forms the highest number of ionic contacts: 46% (Ca^{2+}), 45% (Mg^{2+}), K^+ (42%), and Na^+ (46%). Similarly, as in the case of DPPC, ARG and HIS form only a small number of interactions (1–5%).

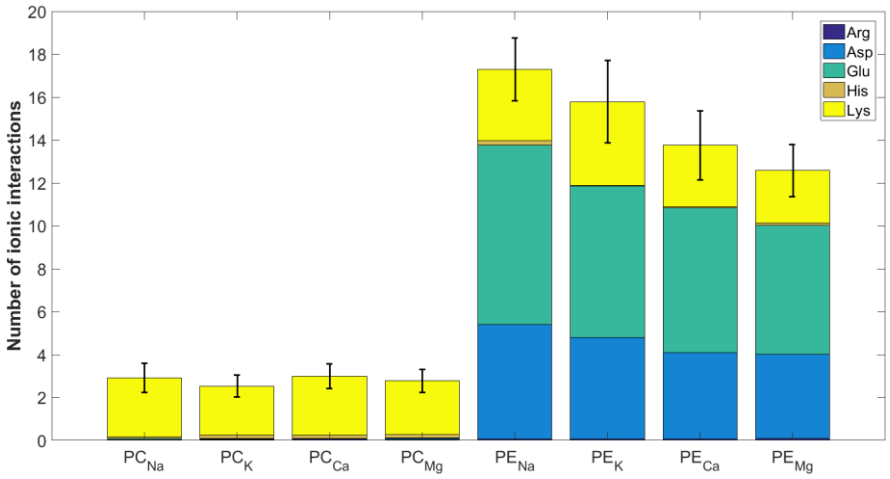

Figure 6. Bar plot showing the average number and standard deviation of direct ionic interactions for all cases studied. The symbols PC and PE represent the phospholipid membranes formed by DPPC and DPPE, respectively.

As presented in Figure 1, HSA bound to the DPPC and DPPE bilayers by domain I and II. However, in the case of DPPE, interactions with domain III also occur (Figure 1C, Tables S1 and S2, Supplementary Materials). The experimental studies of Pantusa et al. [90] showed that the adsorption of DPPC affects the structural features of all domains in HSA. This study, however, does not indicate which parts of albumin interact with a DPPC membrane. It is worth noting that although albumin is negatively charged as a whole molecule under physiological conditions, its polyelectrolytic nature allows it to

contain regions with positive charges. Hence, it can interact with both cationic and anionic surfactants [91]. According to MD simulation results reported by Adamczyk et al. [92], subdomain IA poses the highest negative charge density, while IB and IIIA are positively charged. In particular, the IIIA domain was found to be the most positively charged [92], which makes interaction with the positively charged amino groups of the phospholipid less favorable. Nevertheless, domain III readily interacts with dissolved fatty acids [93–95], suggesting an affinity of this fragment for negatively charged oxygen atoms, which are also present in the phospholipid headgroups. Indeed, as clearly shown in Figure 3C,D, oxygen atoms of the phosphate group in DPPE form intermolecular interactions with the protein. The analysis of ionic molecular contacts reveals that no such interactions are formed by amino acids from domains IIIA and IIIB in the case of DPPC, irrespective of the cation type. HSA interacts with DPPC primarily through domains IA, IIA, and IIB. In the case of domain IA, ionic interactions are formed at 29%, 24%, 23%, and 21% when the complexes contain Ca^{2+}, Mg^{2+}, K^+, and Na^+ ions, respectively. This indicates that Ca^{2+} and Mg^{2+} cations form slightly more ionic contacts with domain IA than K^+ and Na^+ cations. For domain IIA, the highest number of interactions was identified: 46% (Ca^{2+}), 41% (Mg^{2+}), 53% (K^+), and 43% (Na^+). Interestingly, the presence of K^+ cations contributes to the greatest number of interactions involving DPPC. In this case, domain IIB shows no clear preference for cations in terms of the number of ionic contacts formed. This part of albumin is characterized by a negligible number of ionic contacts (1% regardless of the ions contributing to stabilizing the given complex).

In the case of DPPE complexes, ionic interactions were identified in all HSA domains. The highest number of such molecular contacts was identified for domain IA: 29% (Ca^{2+}), 32% (Mg^{2+}), 33% (K^+), and 32% (Na^+), and the lowest for domains IB: 10% (Ca^{2+}), 9% (Mg^{2+}), 10% (K^+), and 9% (Na^+) and IIIA: 12% (Ca^{2+}), 9% (Mg^{2+}), and 8% for the complexes stabilized by Na^+ and K^+. Domain IIIB, in most cases except for the complexes in the presence of K^+, is characterized by a higher percentage of ionic interactions: 16% (Ca^{2+}), 12% (Mg^{2+}), 12% (K^+), and 8% (Na^+). Domain IIA forms fewer interactions than domain IA. For domain IIA, most interactions with DPPE occur in the presence of K^+ and Na^+ (22% and 23%, respectively). The presence of divalent cations causes the formation of slightly fewer ionic contacts: 19% (Ca^{2+}) and 20% (Mg^{2+}).

Similar to previously discussed ionic interactions, DPPE forms more hydrogen bonds with HSA than DPPC (Figure 7). However, this difference is less pronounced. It is worth noting that the methylated ammonium group in DPPC is completely blocked from forming hydrogen bonds. Consequently, hydrogen bonds in DPPC are exclusively formed with oxygen atoms in the phosphate group acting as acceptors. In contrast, DPPE's amine groups can engage in hydrogen bonding with the oxygen atom of the ASP residue ($d = 1.87 \pm 0.15$ Å, Figure 3D). This, in turn, results in enhanced stability of HSA-DPPE complexes relative to those formed with DPPC (Figure 3B).

The contributions of specific HSA domains to hydrogen bond formation are detailed in Table S2 (Supplementary Materials). In complexes formed by DPPC, only IA, IB, and IIB domains participate in hydrogen bonding. Notably, for DPPC/HSA/Mg^{2+} systems, no hydrogen bond interactions with the IB subdomain are detected. In the case of Na^+, $K^{+,}$ and $Ca^{2+,}$ the IB subdomain forms a negligibly small number of intermolecular contacts with DPPC. In contrast, in DPPC/HSA/K^+ complexes, hydrogen bonds involving domain IIA contribute significantly, exceeding 50% of the total interactions. Interestingly, ionic interactions involving domain IIA also account for more than 50% of the total interactions (Table S1, Supplementary Materials). Moreover, in the majority of DPPC complexes, domain IIA likewise forms most of the hydrogen bonds and ionic contacts.

For complexes formed with DPPE, domain IA is the primary contributor to hydrogen bond formation, regardless of the metal ions present in the complexes. Likewise, the DPPC system, the domain responsible for the majority of hydrogen bonds, also forms the most ionic contacts.

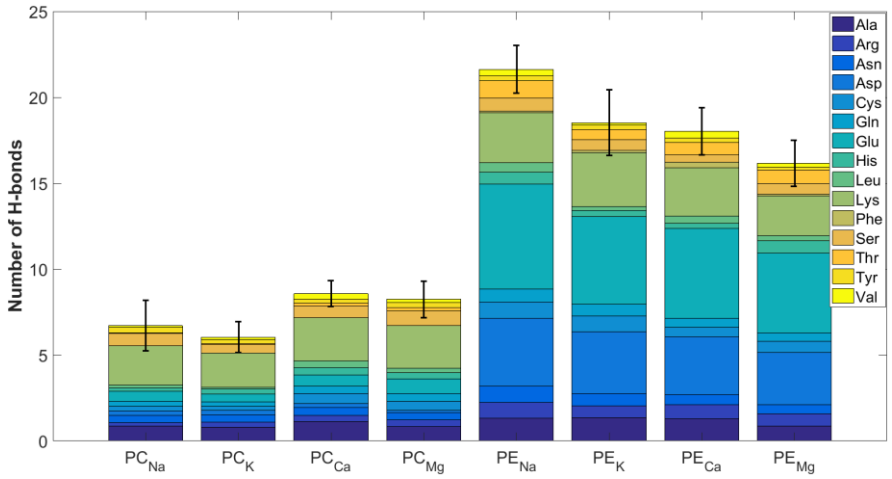

Figure 7. Bar plot showing the average number of hydrogen bonds and their standard deviation for all cases studied. The symbols PC and PE represent the phospholipid membranes formed by DPPC and DPPE, respectively.

The dynamic nature of hydrogen bonding networks in aqueous environments profoundly impacts the behavior of biomolecules. One intriguing aspect of the interactions between phospholipid bilayers and HSA is their impact on biomechanical properties. This includes indirect contacts, such as water bridges. As is well-known, liposomes exhibit excellent lubricating properties. Interestingly, an appropriately large addition of proteins (such as albumin or γ-globulin) to solutions containing phospholipids can lead to an increase in friction between surfaces filled with model synovial fluids [31,96,97]. Low concentrations of albumin can promote lubrication. This suggests a negative impact of forming a dense network of direct interactions between the components on lubricating performance. A significant excess of water relative to the protein is advantageous, as the formation of water bridges between components of the synovial fluid plays a crucial role in reducing friction [98,99]. This is understandable, as effective lubrication at the molecular level is closely linked to the mobility of synovial fluid components.

The structural and energetic details characterizing water bridges are summarized in Table S5 (Supplementary Materials). The majority of hydrogen bonds with water (approximately 80%) are formed by the phospholipid head groups, as expected due to their hydrophilic nature. In the most stable complex examined (DPPE/HSA/Ca^{2+}), the average length of these hydrogen bonds is 1.78 ± 0.20 Å, with a corresponding binding energy of 21.70 ± 4.43 kJ/mol. The higher binding energies, albeit with slightly shorter distances between atoms, are observed for hydrogen bonds connecting the phospholipid and HSA through ASP (E_{bind} = 22.33 ± 3.96 kJ/mol, d = 1.82 ± 0.19 Å), GLU (E_{bind} = 22.26 ± 3.74 kJ/mol, d = 1.82 ± 0.18 Å), GLY (E_{bind} = 21.80 ± 4.01 kJ/mol, d = 1.89 ± 0.16 Å), ILE (E_{bind} = 22.57 ± 2.44 kJ/mol, d = 1.85 ± 0.16 Å), and TRP (E_{bind} = 21.89 ± 3.19 kJ/mol, d = 1.96 ± 0.17 Å). However, the contribution of these interactions is low or negligible (0.02−4.39%). For DPPC, the most stable complex, i.e., the DPPC/HSA/Ca^{2+}, is similarly characterized by high E_{bind} values (18.77−23.28 kJ/mol).

4. Conclusions

In this study, interactions between membranes composed of DPPC and DPPE phospholipids and HSA were analyzed using molecular dynamics. A consequence of protein binding to the membrane is its significant deformation (characteristic curvature). In this way, the system achieves the most energetically favorable organization of phospholipids. This, of course, also indicates the formation of relatively strong interactions between the membrane and HSA, which affect changes in membrane structure. The calculated energy-structural features indicate a high mutual affinity of HSA and studied bilayers. Nevertheless, complexes formed by DPPE are generally more stable than those formed by

DPPC. This is primarily due to differences in the number of ionic contacts and hydrogen bonds. The methylated amine group in DPPC limits the number of possible interactions with HSA, reducing its ability to form stable complexes. Consequently, DPPC forms fewer contacts than DPPE. The other important factor influencing the stability of the considered phospholipid membrane–HSA systems is the presence of mono- and divalent cations. These ions significantly affect the frequency and nature of molecular interactions, such as ionic contacts and hydrogen bonds, between the bilayer and HSA. Nevertheless, DPPE and DPPC differ in how cations affect the stability of their complexes with HSA. Although there is limited experimental data to directly compare with the computational results presented in this study, there are some reports on lecithin that align with the predicted behavior of DPPC bilayers in the presence of Na^+, K^+, and Ca^{2+}.

The results obtained highlight the important role of molecular dynamics in predicting the structure and stability of large biomolecular systems. These insights are crucial for understanding the interactions at the molecular level. Complexes composed of proteins and phospholipids hold substantial biomedical and pharmaceutical potential and are the focus of various research efforts. The observed structural difference between headgroups in DPPE and DPPC affecting the affinity of HSA to the membrane can be useful from the perspective of liposomal technology development, where the phospholipid composition can be precisely tailored to enhance the effectiveness of interactions with target proteins. Furthermore, both HSA and phospholipids are present in synovial fluid, making these insights important for understanding biolubrication mechanisms.

Supplementary Materials: The following supporting information can be downloaded at: https://www.mdpi.com/article/10.3390/app142411753/s1, Figure S1: Snapshot of HSA/membrane/water system simulation box at the end of simulation. Lipid membranes are depicted in pink, HSA in red/green/yellow, and water in the background; Figure S2: Time evolution of last 100 ns of free energy of binding for all complexes; Figure S3: Time evolution of the last 100 ns of free energy of binding for binding sites for all ions; Figure S4: Time evolution of 200 ns of total number of intermolecular ionic interactions between HSA and membrane; Figure S5: Time evolution of 200 ns of the total number of intermolecular hydrogen bonds between HSA and the membrane; Table S1: The percentages of ionic interactions formed by particular residues (top) and HSA domain contributions (bottom); Table S2: The binding energies, distances, and percentages of hydrogen bonds formed by particular HSA domain contributions; Table S3: The percentages, energies, and lengths of hydrogen bonds formed by particular HSA amino acids with the DPPC membrane; Table S4: The percentages, energies, and lengths of hydrogen bonds formed by particular HSA amino acids with the DPPE membrane; Table S5: Hydration of HSA and lipids expressed by the distribution of water bridges stabilizing the DPPC/HSA/Ca^{2+} and DPPE/HSA/Ca^{2+} systems. PHG denotes the phospholipid head group.

Author Contributions: Conceptualization, M.P., P.B. and P.R.; methodology, P.B.; software, P.B., D.L. and Z.L.; validation, M.P., P.B. and P.R.; formal analysis, M.P., P.B., D.L. and Z.L.; investigation, M.P., P.B., P.R., A.D. and P.M.C.; resources, P.B., D.L., Z.L. and A.M.; data curation, P.B.; writing—original draft preparation, M.P., P.B., A.M., A.D. and P.M.C.; writing—review and editing, M.P., P.B., A.M., A.D. and P.M.C.; visualization, P.B.; supervision, M.P., A.D. and P.M.C.; project administration, M.P. All authors have read and agreed to the published version of the manuscript.

Funding: This research received no external funding.

Institutional Review Board Statement: Not applicable.

Informed Consent Statement: Not applicable.

Data Availability Statement: All data supporting the reported results are available on request from the corresponding author.

Conflicts of Interest: The authors declare no conflicts of interest.

References

1. Dai, Y.; Tang, H.; Pang, S. The Crucial Roles of Phospholipids in Aging and Lifespan Regulation. *Front. Physiol.* **2021**, *12*, 775648. [CrossRef]
2. Zachowski, A. Phospholipids in animal eukaryotic membranes: Transverse asymmetry and movement. *Biochem. J.* **1993**, *294*, 1–14. [CrossRef] [PubMed]
3. Scott, H.L.; Bolmatov, D.; Podar, P.T.; Liu, Z.; Kinnun, J.J.; Doughty, B.; Lydic, R.; Sacci, R.L.; Collier, C.P.; Katsaras, J. Evidence for long-term potentiation in phospholipid membranes. *Proc. Natl. Acad. Sci. USA* **2022**, *119*, e2212195119. [CrossRef] [PubMed]
4. Wang, T.; Fei, J.; Dong, Z.; Yu, F.; Li, J. Nanoarchitectonics with a Membrane-Embedded Electron Shuttle Mimics the Bioenergy Anabolism of Mitochondria. *Angew. Chem. Int. Ed.* **2024**, *63*, e202319116. [CrossRef]
5. Herianto, S.; Chien, P.-J.; Ho, J.A.; Tu, H.-L. Liposome-based artificial cells: From gene expression to reconstitution of cellular functions and phenotypes. *Biomater. Adv.* **2022**, *142*, 213156. [CrossRef]
6. Toimil, P.; Prieto, G.; Miñones, J.; Trillo, J.M.; Sarmiento, F. Monolayer and Brewster angle microscopy study of human serum albumin—Dipalmitoyl phosphatidyl choline mixtures at the air–water interface. *Colloids Surf. B Biointerfaces* **2012**, *92*, 64–73. [CrossRef] [PubMed]
7. Nsairat, H.; Khater, D.; Sayed, U.; Odeh, F.; Al Bawab, A.; Alshaer, W. Liposomes: Structure, composition, types, and clinical applications. *Heliyon* **2022**, *8*, e09394. [CrossRef] [PubMed]
8. Makouie, S.; Bryś, J.; Małajowicz, J.; Koczoń, P.; Siol, M.; Palani, B.K.; Bryś, A.; Obranović, M.; Mikolčević, S.; Gruczyńska-Sękowska, E. A Comprehensive Review of Silymarin Extraction and Liposomal Encapsulation Techniques for Potential Applications in Food. *Appl. Sci.* **2024**, *14*, 8477. [CrossRef]
9. De Leo, V.; Maurelli, A.M.; Giotta, L.; Catucci, L. Liposomes containing nanoparticles: Preparation and applications. *Colloids Surf. B Biointerfaces* **2022**, *218*, 112737. [CrossRef]
10. Youness, R.A.; Mohamed, A.H.; Efthimiadou, E.K.; Mekky, R.Y.; Braoudaki, M.; Fahmy, S.A. A Snapshot of Photoresponsive Liposomes in Cancer Chemotherapy and Immunotherapy: Opportunities and Challenges. *ACS Omega* **2023**, *8*, 44424–44436. [CrossRef] [PubMed]
11. Jebastin, K.; Narayanasamy, D. Rationale utilization of phospholipid excipients: A distinctive tool for progressing state of the art in research of emerging drug carriers. *J. Liposome Res.* **2023**, *33*, 1–33. [CrossRef]
12. Ferraz, M.P. Advanced Nanotechnological Approaches for Biofilm Prevention and Control. *Appl. Sci.* **2024**, *14*, 8137. [CrossRef]
13. Qin, S.-S.; Yu, Z.-W.; Yu, Y.-X. Structural and Kinetic Properties of α-Tocopherol in Phospholipid Bilayers, a Molecular Dynamics Simulation Study. *J. Phys. Chem. B* **2009**, *113*, 16537–16546. [CrossRef] [PubMed]
14. Lu, X.; Shi, R.; Hao, C.; Chen, H.; Zhang, L.; Li, J.; Xu, G.; Sun, R. Behavior of lysozyme adsorbed onto biological liquid crystal lipid monolayer at the air/water interface. *Chin. Phys. B* **2016**, *25*, 090506. [CrossRef]
15. Endo, S.; Goss, K.U. Serum albumin binding of structurally diverse neutral organic compounds: Data and models. *Chem. Res. Toxicol.* **2011**, *24*, 2293–2301. [CrossRef]
16. Fasano, M.; Curry, S.; Terreno, E.; Galliano, M.; Fanali, G.; Narciso, P.; Notari, S.; Ascenzi, P. The extraordinary ligand binding properties of human serum albumin. *IUBMB Life* **2005**, *57*, 787–796. [CrossRef]
17. De Simone, G.; Di Masi, A.; Ascenzi, P. Serum albumin: A multifaced enzyme. *Int. J. Mol. Sci.* **2021**, *22*, 10086. [CrossRef] [PubMed]
18. Opriș, O.; Mormile, C.; Lung, I.; Stegarescu, A.; Soran, M.-L.; Soran, A. An Overview of Biopolymers for Drug Delivery Applications. *Appl. Sci.* **2024**, *14*, 1383. [CrossRef]
19. Yang, W.J.; Wu, H.B.; Zhang, C.; Zhong, Q.; Hu, M.J.; He, J.L.; Li, G.A.; Zhu, Z.Y.; Zhu, J.L.; Zhao, H.H.; et al. Exposure to 2,4-dichlorophenol, 2,4,6-trichlorophenol, pentachlorophenol and risk of thyroid cancer: A case-control study in China. *Environ. Sci. Pollut. Res.* **2021**, *28*, 61329–61343. [CrossRef] [PubMed]
20. Neligan, P.J. Fluid and electrolyte balance. *Anaesth. Intensive Care Med.* **2021**, *22*, 169–173. [CrossRef]
21. Maurya, P.; Singh, S.; Mishra, N.; Pal, R.; Singh, N.; Parashar, P.; Saraf, S.A. Albumin-based nanomaterials in drug delivery and biomedical applications. In *Biopolymer-Based Nanomaterials in Drug Delivery and Biomedical Applications*; Elsevier: Amsterdam, The Netherlands, 2021; pp. 465–496.
22. Galántai, R.; Bárdos-Nagy, I. The interaction of human serum albumin and model membranes. *Int. J. Pharm.* **2000**, *195*, 207–218. [CrossRef] [PubMed]
23. Dimitrova, M.N.; Matsumura, H.; Dimitrova, A.; Neitchev, V.Z. Interaction of albumins from different species with phospholipid liposomes. Multiple binding sites system. *Int. J. Biol. Macromol.* **2000**, *27*, 187–194. [CrossRef] [PubMed]
24. de Souza, N.C.; Caetano, W.; Itri, R.; Rodrigues, C.A.; Oliveira, O.N.; Giacometti, J.A.; Ferreira, M. Interaction of small amounts of bovine serum albumin with phospholipid monolayers investigated by surface pressure and atomic force microscopy. *J. Colloid Interface Sci.* **2006**, *297*, 546–553. [CrossRef] [PubMed]
25. Zeno, W.F.; Hilt, S.L.; Risbud, S.H.; Voss, J.C.; Longo, M.L. Lipid Phase Behavior and Protein-Lipid Interactions within Nanolipoprotein Particles upon Sol-Gel Derived Encapsulation. *Biophys. J.* **2016**, *110*, 40a–41a. [CrossRef]
26. Devi, L.S.; Jaiswal, A.K.; Jaiswal, S. Lipid incorporated biopolymer based edible films and coatings in food packaging: A review. *Curr. Res. Food Sci.* **2024**, *8*, 100720. [CrossRef]
27. Mohamed, S.A.A.; El-Sakhawy, M.; El-Sakhawy, M.A.-M. Polysaccharides, Protein and Lipid -Based Natural Edible Films in Food Packaging: A Review. *Carbohydr. Polym.* **2020**, *238*, 116178. [CrossRef]

28. McHugh, T.H. Protein-lipid interactions in edible films and coatings. *Food/Nahr.* **2000**, *44*, 148–151. [CrossRef]
29. Peng, Q.; Wei, X.-Q.; Shao, X.-R.; Zhang, T.; Zhang, S.; Fu, N.; Cai, X.-X.; Zhang, Z.-R.; Lin, Y.-F. Nanocomplex Based on Biocompatible Phospholipids and Albumin for Long-Circulation Applications. *ACS Appl. Mater. Interfaces* **2014**, *6*, 13730–13737. [CrossRef]
30. Mariam, J.; Sivakami, S.; Dongre, P.M. Albumin corona on nanoparticles—A strategic approach in drug delivery. *Drug Deliv.* **2016**, *23*, 2668–2676. [CrossRef]
31. Murakami, T.; Yarimitsu, S.; Nakashima, K.; Sawae, Y.; Sakai, N. Influence of synovia constituents on tribological behaviors of articular cartilage. *Friction* **2013**, *1*, 150–162. [CrossRef]
32. Dėdinaitė, A.; Wieland, D.C.F.; Bełdowski, P.; Claesson, P.M. Biolubrication synergy: Hyaluronan–Phospholipid interactions at interfaces. *Adv. Colloid Interface Sci.* **2019**, *274*, 102050. [CrossRef] [PubMed]
33. Siódmiak, J.; Bełdowski, P.; Augé, W.; Ledziński, D.; Śmigiel, S.; Gadomski, A. Molecular Dynamic Analysis of Hyaluronic Acid and Phospholipid Interaction in Tribological Surgical Adjuvant Design for Osteoarthritis. *Molecules* **2017**, *22*, 1436. [CrossRef] [PubMed]
34. Raczyński, P.; Górny, K.; Bełdowski, P.; Yuvan, S.; Dendzik, Z. Application of Graphene as a Nanoindenter Interacting with Phospholipid Membranes—Computer Simulation Study. *J. Phys. Chem. B* **2020**, *124*, 6592–6602. [CrossRef] [PubMed]
35. Bełdowski, P.; Kruszewska, N.; Yuvan, S.; Dendzik, Z.; Goudoulas, T.; Gadomski, A. Capstan-like mechanism in hyaluronan–phospholipid systems. *Chem. Phys. Lipids* **2018**, *216*, 17–24. [CrossRef] [PubMed]
36. Bełdowski, P.; Yuvan, S.; Dėdinaitė, A.; Claesson, P.M.; Pöschel, T. Interactions of a short hyaluronan chain with a phospholipid membrane. *Colloids Surf. B Biointerfaces* **2019**, *184*, 110539. [CrossRef] [PubMed]
37. Raczyński, P.; Górny, K.; Bełdowski, P.; Marciniak, B.; Pöschel, T.; Dendzik, Z. Influence of silicon nanocone on cell membrane self-sealing capabilities for targeted drug delivery—Computer simulation study. *Arch. Biochem. Biophys.* **2023**, *749*, 109802. [CrossRef]
38. Bełdowski, P.; Przybyłek, M.; Raczyński, P.; Dedinaite, A.; Górny, K.; Wieland, F.; Dendzik, Z.; Sionkowska, A.; Claesson, P.M. Albumin–Hyaluronan Interactions: Influence of Ionic Composition Probed by Molecular Dynamics. *Int. J. Mol. Sci.* **2021**, *22*, 12360. [CrossRef]
39. Arias-Moreno, X.; Abian, O.; Vega, S.; Sancho, J.; Velazquez-Campoy, A. Protein-Cation Interactions: Structural and Thermodynamic Aspects. *Curr. Protein Pept. Sci.* **2011**, *12*, 325–338. [CrossRef] [PubMed]
40. Singh, A.; Maity, A.; Singh, N. Structure and Dynamics of dsDNA in Cell-like Environments. *Entropy* **2022**, *24*, 1587. [CrossRef] [PubMed]
41. Sarkar, R.; Mainan, A.; Roy, S. Influence of ion and hydration atmospheres on RNA structure and dynamics: Insights from advanced theoretical and computational methods. *Chem. Commun.* **2024**, *60*, 3624–3644. [CrossRef]
42. Bonté, F.; Juliano, R.L. Interactions of liposomes with serum proteins. *Chem. Phys. Lipids* **1986**, *40*, 359–372. [CrossRef] [PubMed]
43. Petrache, H.I.; Tristram-Nagle, S.; Harries, D.; Kučerka, N.; Nagle, J.F.; Parsegian, V.A. Swelling of phospholipids by monovalent salt. *J. Lipid Res.* **2006**, *47*, 302–309. [CrossRef]
44. Cordomí, A.; Edholm, O.; Perez, J.J. Effect of Ions on a Dipalmitoyl Phosphatidylcholine Bilayer. A Molecular Dynamics Simulation Study. *J. Phys. Chem. B* **2008**, *112*, 1397–1408. [CrossRef] [PubMed]
45. Gurtovenko, A.A.; Vattulainen, I. Ion Leakage through Transient Water Pores in Protein-Free Lipid Membranes Driven by Transmembrane Ionic Charge Imbalance. *Biophys. J.* **2007**, *92*, 1878–1890. [CrossRef] [PubMed]
46. Tantipolphan, R.; Rades, T.; McQuillan, A.J.; Medlicott, N.J. Adsorption of bovine serum albumin (BSA) onto lecithin studied by attenuated total reflectance Fourier transform infrared (ATR-FTIR) spectroscopy. *Int. J. Pharm.* **2007**, *337*, 40–47. [CrossRef] [PubMed]
47. Kitaoka, H.; Yokoyama, Y.; Sakka, T.; Nishi, N. Salting-out and Competitive Adsorption of Ethanol into Lipid Bilayer Membranes: Conflicting Effects of Salts on Ethanol–Membrane Interactions Studied by Molecular Dynamics Simulations. *J. Phys. Chem. B* **2024**, *128*, 7596–7604. [CrossRef] [PubMed]
48. Duan, Y.; Wu, C.; Chowdhury, S.; Lee, M.C.; Xiong, G.; Zhang, W.; Yang, R.; Cieplak, P.; Luo, R.; Lee, T.; et al. A Point-Charge Force Field for Molecular Mechanics Simulations of Proteins Based on Condensed-Phase Quantum Mechanical Calculations. *J. Comput. Chem.* **2003**, *24*, 1999–2012. [CrossRef]
49. Burley, S.K.; Berman, H.M.; Bhikadiya, C.; Bi, C.; Chen, L.; Di Costanzo, L.; Christie, C.; Duarte, J.M.; Dutta, S.; Feng, Z.; et al. Protein Data Bank: The single global archive for 3D macromolecular structure data. *Nucleic Acids Res.* **2019**, *47*, D520–D528.
50. Krieger, E.; Vriend, G. YASARA View—Molecular graphics for all devices—From smartphones to workstations. *Bioinformatics* **2014**, *30*, 2981–2982. [CrossRef]
51. Jo, S.; Kim, T.; Im, W. Automated Builder and Database of Protein/Membrane Complexes for Molecular Dynamics Simulations. *PLoS ONE* **2007**, *2*, e880. [CrossRef] [PubMed]
52. Jo, S.; Vargyas, M.; Vasko-Szedlar, J.; Roux, B.; Im, W. PBEQ-Solver for online visualization of electrostatic potential of biomolecules. *Nucleic Acids Res.* **2008**, *36*, W270–W275. [CrossRef]
53. Jo, S.; Kim, T.; Iyer, V.G.; Im, W. CHARMM-GUI: A web-based graphical user interface for CHARMM. *J. Comput. Chem.* **2008**, *29*, 1859–1865. [CrossRef] [PubMed]
54. Jorgensen, W.L. Quantum and statistical mechanical studies of liquids. 10. Transferable intermolecular potential functions for water, alcohols, and ethers. Application to liquid water. *J. Am. Chem. Soc.* **1981**, *103*, 335–340. [CrossRef]

55. Mark, P.; Nilsson, L. Structure and dynamics of the TIP3P, SPC, and SPC/E water models at 298 K. *J. Phys. Chem. A* **2001**, *105*, 9954–9960. [CrossRef]
56. Essmann, U.; Perera, L.; Berkowitz, M.L.; Darden, T.; Lee, H.; Pedersen, L.G. A smooth particle mesh Ewald method. *J. Chem. Phys.* **1995**, *103*, 8577–8593. [CrossRef]
57. Schuler, L.D.; Daura, X.; Van Gunsteren, W.F.; Rapold, R.F.; Suter, U.W.; Darden, T.T.A.; York, D.; Pedersen, L.G.; Fuchs, P.F.J.; Hansen, H.S.; et al. Molecular dynamics with coupling to an external bath. *J. Chem. Phys.* **2001**, *81*, 3586–3616.
58. Genheden, S.; Ryde, U. The MM/PBSA and MM/GBSA methods to estimate ligand-binding affinities. *Expert Opin. Drug Discov.* **2015**, *10*, 449–461. [CrossRef]
59. Holst, M.; Baker, N.; Wang, F. Adaptive multilevel finite element solution of the Poisson-Boltzmann equation I. Algorithms and examples. *J. Comput. Chem.* **2000**, *21*, 1319–1342. [CrossRef]
60. Krieger, E.; Vriend, G. New ways to boost molecular dynamics simulations. *J. Comput. Chem.* **2015**, *36*, 996–1007. [CrossRef]
61. Krieger, E.; Dunbrack, R.L.; Hooft, R.W.W.; Krieger, B. Assignment of Protonation States in Proteins and Ligands: Combining pKa Prediction with Hydrogen Bonding Network Optimization. In *Computational Drug Discovery and Design*; Springer: New York, NY, USA, 2012; pp. 405–421.
62. Leekumjorn, S.; Sum, A.K. Molecular studies of the gel to liquid-crystalline phase transition for fully hydrated DPPC and DPPE bilayers. *Biochim. Biophys. Acta -Biomembr.* **2007**, *1768*, 354–365. [CrossRef]
63. Brown, M.F. Curvature forces in membrane lipid–protein interactions. *Biochemistry* **2012**, *51*, 9782–9795. [CrossRef] [PubMed]
64. Pérez-Isidoro, R.; Díaz-Salazar, A.J.; Costas, M. Biophysical study of the effect of ovalbumin and lysozyme in DMPC/sphingomyelin/cholesterol bilayers. *J. Therm. Anal. Calorim.* **2024**, *149*, 1219–1229. [CrossRef]
65. Khodam Hazrati, M.; Vácha, R. Membrane Adsorption Enhances Translocation of Antimicrobial Peptide Buforin 2. *J. Phys. Chem. B* **2024**, *128*, 8469–8476. [CrossRef] [PubMed]
66. Nylund, M.; Fortelius, C.; Palonen, E.K.; Molotkovsky, J.G.; Mattjus, P. Membrane curvature effects on glycolipid transfer protein activity. *Langmuir* **2007**, *23*, 11726–11733. [CrossRef] [PubMed]
67. Jones, M.N. Surfactants in membrane solubilisation. *Int. J. Pharm.* **1999**, *177*, 137–159. [CrossRef] [PubMed]
68. Richardson, J.D.; Van Lehn, R.C. Free Energy Analysis of Peptide-Induced Pore Formation in Lipid Membranes by Bridging Atomistic and Coarse-Grained Simulations. *J. Phys. Chem. B* **2024**, *128*, 8737–8752. [CrossRef] [PubMed]
69. Meyuhas, D.; Lichtenberg, D. The effect of albumin on the state of aggregation and phase transformations in phosphatidylcholine-sodium cholate mixtures. *Biochim. Biophys. Acta -Biomembr.* **1995**, *1234*, 203–213. [CrossRef] [PubMed]
70. Al-Ayed, M.S. Biophysical studies on the liposome-albumin system. *Indian J. Biochem. Biophys.* **2006**, *43*, 186–189.
71. Rivel, T.; Ramseyer, C.; Yesylevskyy, S. The asymmetry of plasma membranes and their cholesterol content influence the uptake of cisplatin. *Sci. Rep.* **2019**, *9*, 5627. [CrossRef] [PubMed]
72. Melcrová, A.; Pokorna, S.; Vošahlíková, M.; Sýkora, J.; Svoboda, P.; Hof, M.; Cwiklik, L.; Jurkiewicz, P. Concurrent Compression of Phospholipid Membranes by Calcium and Cholesterol. *Langmuir* **2019**, *35*, 11358–11368. [CrossRef]
73. Wiig, H.; Kolmannskog, O.; Tenstad, O.; Bert, J.L. Effect of charge on interstitial distribution of albumin in rat dermis in vitro. *J. Physiol.* **2003**, *550*, 505–514. [CrossRef] [PubMed]
74. Jachimska, B.; Pajor, A. Physico-chemical characterization of bovine serum albumin in solution and as deposited on surfaces. *Bioelectrochemistry* **2012**, *87*, 138–146. [CrossRef] [PubMed]
75. Huang, P.; Loew, G.H. Interaction of an Amphiphilic Peptide with a Phospholipid Bilayer Surface by Molecular Dynamics Simulation Study. *J. Biomol. Struct. Dyn.* **1995**, *12*, 937–956. [CrossRef] [PubMed]
76. Balali-Mood, K.; Bond, P.J.; Sansom, M.S.P. Interaction of monotopic membrane enzymes with a lipid bilayer: A coarse-grained MD simulation study. *Biochemistry* **2009**, *48*, 2135–2145. [CrossRef]
77. Mansourian, M.; Mahnam, K.; Madadkar-Sobhani, A.; Fassihi, A.; Saghaie, L. Insights into the human A1 adenosine receptor from molecular dynamics simulation: Structural study in the presence of lipid membrane. *Med. Chem. Res.* **2015**, *24*, 3645–3659. [CrossRef]
78. Gedeon, P.C.; Indarte, M.; Surratt, C.K.; Madura, J.D. Molecular dynamics of leucine and dopamine transporter proteins in a model cell membrane lipid bilayer. *Proteins Struct. Funct. Bioinform.* **2010**, *78*, 797–811. [CrossRef]
79. Yi, X.; Zhang, Y.; Gong, M.; Yu, X.; Darabedian, N.; Zheng, J.; Zhou, F. Ca^{2+} Interacts with Glu-22 of Aβ(1–42) and Phospholipid Bilayers to Accelerate the Aβ(1–42) Aggregation Below the Critical Micelle Concentration. *Biochemistry* **2015**, *54*, 6323–6332. [CrossRef] [PubMed]
80. Sahu, S.K.; Aradhyam, G.K.; Gummadi, S.N. Calcium binding studies of peptides of human phospholipid scramblases 1 to 4 suggest that scramblases are new class of calcium binding proteins in the cell. *Biochim. Biophys. Acta -Gen. Subj.* **2009**, *1790*, 1274–1281. [CrossRef]
81. Filoteo, A.G.; Enyedi, A.; Penniston, J.T. The lipid-binding peptide from the plasma membrane Ca^{2+} pump binds calmodulin, and the primary calmodulin-binding domain interacts with lipid. *J. Biol. Chem.* **1992**, *267*, 11800–11805. [CrossRef] [PubMed]
82. Mohan, M.S.; Bates, R.G.; Hiller, J.M.; Brand, M.J. Measurement of sodium in albumin solutions with ion-selective electrodes. *Clin. Chem.* **1978**, *24*, 580–584. [CrossRef] [PubMed]
83. Van Os, G.A.J.; Koopman-van Eupen, J.H.M. The interaction of sodium, potassium, calcium, and magnesium with human serum albumin, studied by means of conductivity measurements. *Recl. Trav. Chim. Pays-Bas* **1957**, *76*, 390–400. [CrossRef]

84. Liu, C.; Min, F.; Liu, L.; Chen, J.; Ren, B.; Lv, K.; Tan, Y. Experimental study on the effect of ions on the surface hydration characteristics of fine quartz. *Physicochem. Probl. Miner. Process.* **2022**, *58*, 150280. [CrossRef]
85. Hills, B.A. *The Biology of Surfactant*; Cambridge University Press: Cambridge, UK; New York, NY, USA; New Rochelle, NY, USA; Melbourne, Australia; Sidney, Australia, 1988.
86. Cho, D.; Narsimhan, G.; Franses, E.I. Interactions of Spread Lecithin Monolayers with Bovine Serum Albumin in Aqueous Solution. *Langmuir* **1997**, *13*, 4710–4715. [CrossRef]
87. Phang, T.-L.; Franses, E.I. Expulsion of bovine serum albumin from the air/water interface by a sparingly soluble lecithin lipid. *J. Colloid Interface Sci.* **2004**, *275*, 477–487. [CrossRef] [PubMed]
88. Conti Nibali, V.; Branca, C.; Wanderlingh, U.; D'Angelo, G. Intermolecular Hydrogen-Bond Interactions in DPPE and DMPC Phospholipid Membranes Revealed by Far-Infrared Spectroscopy. *Appl. Sci.* **2021**, *11*, 10038. [CrossRef]
89. Leekumjorn, S.; Sum, A.K. Molecular investigation of the interactions of trehalose with lipid bilayers of DPPC, DPPE and their mixture. *Mol. Simul.* **2006**, *32*, 219–230. [CrossRef]
90. Pantusa, M.; Sportelli, L.; Bartucci, R. Spectroscopic and calorimetric studies on the interaction of human serum albumin with DPPC/PEG:2000-DPPE membranes. *Eur. Biophys. J.* **2008**, *37*, 961–973. [CrossRef]
91. Liu, Y.; Cao, Z.; Wang, J.; Zong, W.; Liu, R. The interaction mechanism between anionic or cationic surfactant with HSA by using spectroscopy, calorimetry and molecular docking methods. *J. Mol. Liq.* **2016**, *224*, 1008–1015. [CrossRef]
92. Adamczyk, O.; Szota, M.; Rakowski, K.; Prochownik, M.; Doveiko, D.; Chen, Y.; Jachimska, B. Bovine Serum Albumin as a Platform for Designing Biologically Active Nanocarriers—Experimental and Computational Studies. *Int. J. Mol. Sci.* **2023**, *25*, 37. [CrossRef] [PubMed]
93. Michnik, A. Thermal stability of bovine serum albumin DSC study. *J. Therm. Anal. Calorim.* **2003**, *71*, 509–519. [CrossRef]
94. Curry, S. Plasma albumin as a fatty acid carrier. *Adv. Mol. Cell Biol.* **2003**, *33*, 29–46.
95. Hamilton, J.A.; Era, S.; Bhamidipati, S.P.; Reed, R.G. Locations of the three primary binding sites for long-chain fatty acids on bovine serum albumin. *Proc. Natl. Acad. Sci. USA* **1991**, *88*, 2051–2054. [CrossRef] [PubMed]
96. Yarimitsu, S.; Nakashima, K.; Sawae, Y.; Murakami, T. Influence of phospholipid and protein constituents on tribological properties of artificial hydrogel cartilage material. *J. Biomech. Sci. Eng.* **2013**, *8*, 257–267. [CrossRef]
97. Krishna, D.V.; Sankar, M.R. Bioinspired artificial synovial fluid for in vitro frictional behavior of bovine articular cartilage and auxiliary biomaterials. *J. Mol. Liq.* **2023**, *388*, 122836. [CrossRef]
98. Janicka, K.; Beldowski, P.; Majewski, T.; Urbaniak, W.; Petelska, A.D. The Amphoteric and Hydrophilic Properties of Cartilage Surface in Mammalian Joints: Interfacial Tension and Molecular Dynamics Simulation Studies. *Molecules* **2019**, *24*, 2248. [CrossRef]
99. Chatterjee, A.; Dubey, D.K.; Sinha, S.K. Nanoscale friction and adhesion mechanisms in articular cartilage top layer hydrated interfaces: Insights from atomistic simulations. *Appl. Surf. Sci.* **2021**, *550*, 149216. [CrossRef]